ISSN 2004-2965 Energy Proceedings, Vol. 21, 2021

International Conference on Applied Energy 2021
Nov. 29 - Dec. 5, 2021, Thailand/Virtual
Paper ID: 0427

Segmented Thermoelectric Generator Modeling Using Artificial Neural Networks

Yuxiao Zhu*, Daniel W. Newbrook, Peng Dai, C. H. (Kees) de Groot
and Ruomeng Huang
School of Electronics and Computer Science, University of Southampton, Southampton, United Kingdom

ABSTRACT

With the goal of net-zero expected to be accomplished in recent decades, the development of a thermoelectric generator, one of the energy harvesting technologies, is important. Along with efforts to discover more cost-effective thermoelectric materials, geometric and structural optimization of thermoelectric generators is essential to maximize power and efficiency. This work demonstrates a segmented thermoelectric generator, one of the advanced structures of a thermoelectric generator, modeling using artificial neural networks. After training the artificial neural networks, we have achieved 98.9% accuracy compared to COMSOL simulation results under constant temperature difference while speeding up the computational speed over a few thousand times. This new approach illustrates the advantages of the modeling of segmented thermoelectric generators.

Keywords: Artificial neural network, segmented thermoelectric generator, modeling

1. INTRODUCTION

The importance of renewable energy and energy harvesting is increasingly attracting the attention of society. In 2021, the International Energy Agency, together with several countries, set the goal of achieving net-zero by 2050 [1]. This renders a significant challenge in the development of novel clean renewable energies that can be harvested to replace conventional fossil-based energy. Traditional forms of energy (e.g., fossil energy) have a conversion rate of less than 50%, a large proportion of which is lost in the form of heat.

A thermoelectric generator (TEG) is a device that can harvest thermal energy and convert it into electricity. Research into this type of renewable energy is therefore important to achieve net-zero and reduce dependence on fossil fuels. TEGs are based on the Seebeck effect, when heat is applied to the n-type material and p-type material, electric current will be generated. So by using this effect and placing the two materials thermally in parallel but electrically in series, a current can be generated within the thermoelectric generator [2]. Current research of TEGs normally falls into two main areas, thermoelectric materials improvement, and TEG structure optimization. Research on materials is mainly focused on developing materials with high figure-of-merit (ZT). The latest research has led to many breakthroughs in materials. For example, SnSe [3], PbTe [4] achieves ZT greater than 2 at high temperatures, usually over 600K, and other lower temperatures materials, e.g. $Bi_2Te_{2.7}Se_{0.3}$ [5] (ZT=1.04@400K).

Nonetheless, obtaining high ZT thermoelectric materials will not guarantee a high TEG power performance. To transfer the high thermoelectric properties into power generation, the structure of the thermoelectric generator needs to be developed and optimized for it to work at its optimum level. TEG with segmented thermoelectric legs has been proposed [6]. By joining thermoelectric materials with high ZT values in different temperature ranges in one leg, the segmented-TEG (STEG) can significantly improve the power performance especially at the condition where the temperature gradient across the TEG is large. However, optimization of STEG can be challenging due to the complex interaction between different geometrical parameters (e.g., leg dimension, fill factor), temperature-dependent thermoelectric properties (e.g., Seebeck coefficient, thermal/electrical conductivity), and complicated thermoelectric phenomena (e.g., Thompson effect). For each optimization, a TEG model

Selection and peer-review under responsibility of the scientific committee of the 13th Int. Conf. on Applied Energy (ICAE2021).

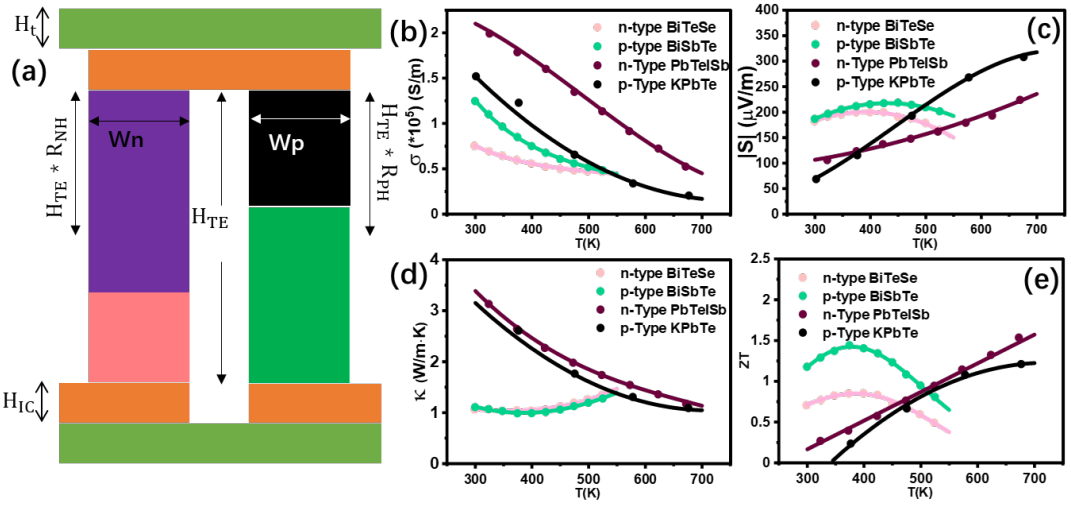

Fig. 1. (a) Schematic of Segmented TEG. (b) Electrical conductivity, (c) Seebeck coefficient, (d) thermal conductivity and (e) ZT in STEG.

that can accurately reflect the relation between parameter and power performance needs to be first developed. The most common way of modeling is by simplifying physical processes and summarising mathematical formulas. For example, Kim et al. developed a simplified mathematical model for a STEG [7]. Zhu et al. reported a mathematical model even more accurate by simplifying the thermoelectric generator to a 1-D model, specializing in the variation of parameters on the legs of STEGs [8]. However, the accuracies of these mathematical models are often limited because several physical factors are ignored in the modeling. 3D TEG finite element models enabled by commercial software (e.g. COMSOL and ANSYS) can consider all thermoelectric factors and environmental conditions and achieve accurate TEG power performance prediction [9]. Yet using that software is extremely dependent on computational resources and can be time-consuming.

Artificial neural network (ANN) is one of the structures in deep learning [10]. The basic structure of ANN is a neuron. It simulates the real neuron in biology. By combining many neurons, the network can process a large amount of information. The network is then brought close to the target by a gradient descent algorithm. Such networks rely on the complexity of the system to process information by adapting the relationships between the large number of nodes interconnected within it. Recently, ANNs have been used in a wide variety of fields, such as image recognition [11], nano-photonics[?]. More importantly, ANN can find patterns in massive data that are normally difficult for researchers to figure out. By training using a pre-generated dataset, it is possible to model directly, bypassing complex physical definitions, and then explore the physical meaning in the physical model. It is therefore very suitable for the study of TEGs. Our group has recently developed a set of ANNs that enable accurate modeling of conventional bulk TEG under different operating conditions [12]. The superiority of ANN for modeling bulk TEGs is demonstrated through accuracy of 98% but with computational efficiency over 1000 times higher than COMSOL simulations. This ANN model has an accuracy close to that of the finite element analysis method, as well as an ultra-fast computing speed, so we have further extended this method to the more complex TEG model, the segmented TEG.

In this work, we further explored the modeling of the complicated STEG structure using ANN under constant temperature differences. The ANN will be first developed through a training process with a dataset generated from 3-D COMSOL simulation. The prediction performance such as accuracy and efficiency of the trained ANN will be presented and compared with the simulated results.

2. METHOD

2.1 Physical model and parameters description

Fig. 1a shows the STEG model investigated in this work. The green part represents the AlN ceramic layer. For n-type leg, $PbTe_{0.998}I_{0.002}$-3%Sb [13] was selected as the high-temperature material (purple) and $Bi_2Te_{2.7}Se_{0.3}$ [5] was selected as low-temperature material (pink). For p-type leg, $K_{0.02}Pb_{0.98}Te$ (black) [14] and $Bi_{0.5}$ $Sb_{1.5}Te_3$ (green) [15] were selected as high and low temperature materials, respectively. These materials were developed from past studies where the temperature-dependent properties are shown in fig. 1b-1e. The electrode (yellow) is made of copper.

The ranges of all parameters that need to be optimized are shown in Table.1. These parameters are divided into two categories: geometrical parameters and operating conditions. The geometrical parameters include the leg height of STEG H_{TE}, FF, n-type high-temperature material height ratio R_{NH}, and p-type high-temperature material height ratio R_{PH}. The working conditions include the temperature of the hot side T_h, and the contact resistivity of the upper ρ_{tC} and lower surfaces ρ_{bC}. In this work, FF is defined as the sum of the n-type leg and p-type leg areas divided by the ceramic layer area. And the n-type leg and the p-type leg have the same width. The area of the ceramic layer is fixed at 100 mm^2. The remaining parameters are used as constants, $H_{IC} = 0.5\ mm, H_t = 0.5\ mm$ and the Cold-side temperature is fixed at 300K.

Table.1 Parameters in Segemented TEG

Geometrical Parameter	**Value Range**
Height of the TEG leg ($\mathrm{H_{TE}}$)	1 – 10 mm
Filling Factor (FF)	0.05 – 0.95
High Temperature n-type TEG leg height ratio ($\mathrm{R_{NH}}$)	0.05 – 0.95
High Temperature p-type TEG leg height ratio ($\mathrm{R_{PH}}$)	0.05 – 0.95
Operation Condition	**Value Range**
Hot-side temperature ($\mathrm{T_h}$)	400 – 700 K
Top side contact resistivity ($\boldsymbol{\rho}_{\mathrm{tc}}$)	10^{-9}– $10^{-7}\Omega \cdot m^2$
Bottom side contact resistivity ($\boldsymbol{\rho}_{\mathrm{bc}}$)	10^{-9}– $10^{-7}\Omega \cdot m^2$

2.2 Dataset Generation and ANN Training

Once all the parameters of the segmented TEG have been determined, the output power and efficiency of the TEG can be simulated using 3D finite element analysis software to generate the dataset for ANN training. The software used in this work is COMSOL Multiphysics. 5000 sets of inputs including both geometrical parameter and operating condition list in Table 1 were randomly generated with uniform distribution. These inputs were then simulated in COMSOL to obtain the output power and efficiency. This dataset was split into groups of 4000, 500, and 500 for training, validation, and the test, respectively.

Fig.2a displays the simple structure of an ANN with 7 input parameters, divided into geometrical parameters and operating conditions according to the classification in Table. 1. Hidden layers are 5-layer structures with 200 neurons per layer. The two outputs of the ANN are the maximum output power density (PD_{max}) and efficiency. Fig.2b is a display of the training loss (i.e., mean square error) as a function of the training epoch. The mean square error between the real results (simulated by COMSOL) and the ANN predicted results are used for backpropagation to update the weights and bias in each neuron. In general, the whole curve shows a downward trend, which means that ANN is slowly finding the best values as it back propagates. Around the 1900 epoch, the overall ANN has reached a relatively optimal state. All ANN training code is written in Python, using the Pytorch module.

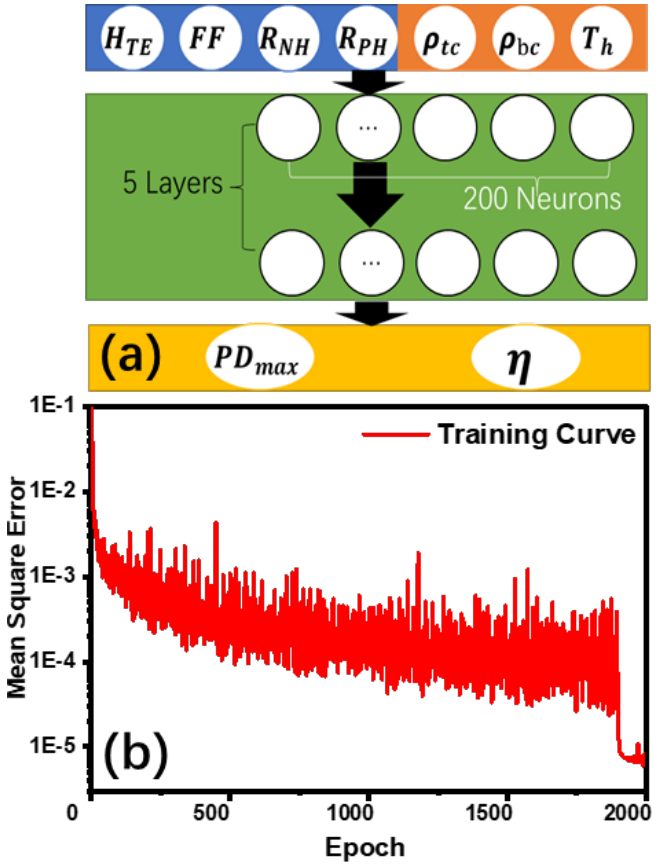

Fig. 2. (a) ANN structure and hyperparameters. (b) Training loss of ANN.

2.3 Results and discussion

Fig.3a shows the test results of the ANN. The horizontal and vertical coordinates are the PD_{max} of the COMSOL simulation and ANN predictions respectively. The red line is the y=x fit through all points. R^2 is the goodness of fit, which measures the accuracy of the fit. Here we obtain an R^2 value of 0.99944, indicating a good match with the ANN and COMSOL results and for the efficiency results, the goodness of fit is even better. To measure the

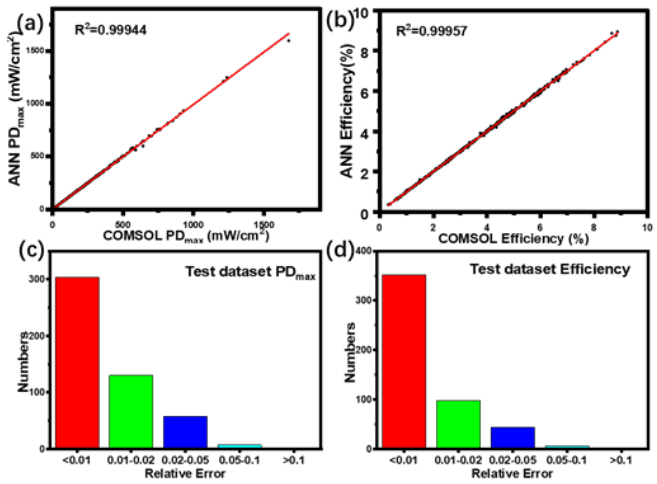

Fig. 3. Test results of the ANN and the COMSOL (a) PD_{max}. (b) efficiency. (c) The distribution of test data relative error on (c) PD_{max} and (d) effciency.

accuracy of the ANN, the concept of relative error rate is introduced here: $Relative\ Error = |Result_{ANN} - Result_{COMSOL}|/Result_{COMSOL}$. On this basis, the accuracy can be expressed as $Accuracy = 1 - Relative\ Error$. Fig.3c shows the distribution of relative errors in the test data. From the figure over 60% of the data has a relative error of less than 1%, while only 1.6% of the data has a relative error rate of 5% or more. The average relative error in the overall test data is 0.011, meaning that ANN's accuracy rate is approximately 98.9%. Same in the distribution of efficiency in Fig. 4d. More importantly, this highly accurate modeling can be achieved within milliseconds in a single test, which is over 10000 times quicker than the time required for COMSOL simulation $(90 \pm 30s)$. These results suggest that ANNs can achieve accuracy close to that of COMSOL simulation, while significantly saving time and computational resources.

By using the accurate ANN STEG model, the effect of all parameters on the STEG can be investigated. As an example, we will demonstrate, in Fig. 4, the effect of the high-temperature material height ratio R_{NH} under different hot-side temperatures with other parameters remains fixed. The operating condition chosen is ρ_{bc} and ρ_{tc} of 10^{-8} Ω·m^2. The H_{TE}, FF and R_{PH} values were fixed at 5 mm, 0.5, and 0.5, respectively. Fig 4b is the corresponding efficiency results. In Fig. 4, the lines are the data generated by the ANN and the triangles are the data from the COMSOL simulation. When the temperature difference is fixed, PD_{max} firstly increases and then decreases with R_{NH}, which would indicate that the segmented structure has a higher output power than a single material TEG at that conditions. When the temperature is fixed, increasing the ratio of high-temperature material from start will cause more high-temperature material to work in the higher temperature region, which will generate more voltage in comparison to the medium and low-temperature material, increasing power. As the ratio of high-temperature material increases further, more high-temperature material enters the low-temperature region, generating less voltage compared to the original medium to low-temperature material, leading to a reduction in power.

The blue dots in Fig. 4 represent the optimized ratio for different operating temperatures. The higher the temperature, the greater the R_{NH} at which the peak of PD_{max} occurs. This can be explained by the fact that as the temperature increases, the distribution of high-temperature regions over the STEG legs increase. In turn, the use of high-temperature materials in these high-

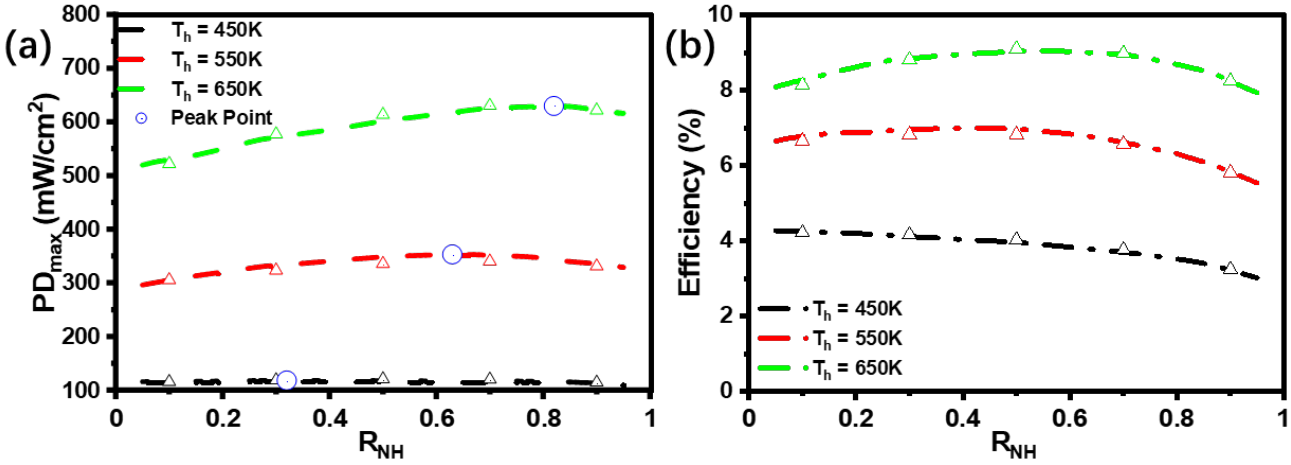

Fig. 4 (a)PD_{max} and (b)efficiency obtained from ANN (line) and COMSOL simulation (triangles) as a function of R_{NH} and T_h. The operating condition chosen is ρ_{bC} and ρ_{tC} of 10^{-8} Ω·m^2. The H_{TE}, FF and R_{PH} values were fixed at 5 mm, 0.5 and 0.5, respectively. Blue dots are the peak of PD_{max}

temperature regions generates more power than medium to low-temperature materials. Therefore, the ratio of high-temperature materials that show peaks increases as the temperature increases. This is very much in line with the common perception of STEG, and the fact that ANN can show these patterns without knowing any preconception reinforces the superiority of ANN modeling.

3. CONCLUSIONS

In conclusion, this work reports the forward modeling of segmented TEG using an artificial neural network. After training the overall ANN model demonstrates accuracy close to 99%, compared to the COMSOL simulation results under constant temperature difference. Also, several thousand times faster than COMSOL simulation is achieved through ANN, which means the computational efficiency is significantly improved. Compared to the other mathematical modeling, no prior knowledge is required in ANN modeling and can still ensure accuracy. In addition, ANN can consider more complex variables which normal mathematic models usually have to ignore.

The development of such an ANN model that enables accurate and fast prediction of the complex relationships between the STEG parameters and power performance will further facilitate the STEG design optimization by coupling the model with optimization techniques (e.g., evolutionary optimization).

REFERENCE{BIBLIOGRAPHY}

[1] IEA (2021), Global Energy Review 2021, https://www.iea.org/reports/global-energy-review-2021. Paris: 2021.

[2] Snyder GJ, Toberer ES. Complex thermoelectric materials. Nat Mater 2008;7:105–14.

[3] Duong AT, Nguyen VQ, Duvjir G, Duong VT, Kwon S, Song JY, et al. Achieving ZT=2.2 with Bi-doped n-type SnSe single crystals. Nat Commun 2016;7:1–6.

[4] Tan G, Shi F, Hao S, Zhao L-D, Chi H, Zhang X, et al. Non-equilibrium processing leads to record high thermoelectric figure of merit in PbTe–SrTe. Nat Commun 2016;7:12167.

[5] Yan X, Poudel B, Ma Y, Liu WS, Joshi G, Wang H, et al. Experimental studies on anisotropic thermoelectric properties and structures of n-type Bi2Te2.7Se0.3. Nano Lett 2010;10:3373–8.

[6] Crane DT. An introduction to system-level, steady-state and transient modeling and optimization of high-power-density thermoelectric generator devices made of segmented thermoelectric elements. J Electron Mater 2011;40:561–9.

[7] Kim HS, Kikuchi K, Itoh T, Iida T, Taya M. Design of segmented thermoelectric generator based on cost-effective and light-weight thermoelectric alloys. Mater Sci Eng B Solid-State Mater Adv Technol 2014;185:45–52.

[8] Zhu L, Li H, Chen S, Tian X, Kang X, Jiang X, et al. Optimization analysis of a segmented thermoelectric generator based on genetic algorithm. Renew Energy 2020;156:710–8.

[9] Shittu S, Li G, Zhao X, Ma X, Akhlaghi YG, Ayodele E. High performance and thermal stress analysis of a segmented annular thermoelectric generator. Energy Convers Manag 2019;184:180–93.

[10] Lecun Y, Bengio Y, Hinton G. Deep learning. Nature 2015;521:436–44.

[11] Wang S-C. Artificial Neural Network. Interdiscip. Comput. Java Program., Boston, MA: Springer US; 2003, p. 81–100.

[12] Zhu Y, Newbrook DW, Dai P, Groot CHK De. Artificial neural network enabled accurate geometrical design and optimisation of thermoelectric generator. Appl Energy 2022;305:117800.

[13] Fu L, Yin M, Wu D, Li W, Feng D, Huang L, et al. Large enhancement of thermoelectric properties in n-type PbTe via dual-site point defects. Energy Environ Sci 2017;10:2030–40.

[14] Zhang Q, Cao F, Liu W, Lukas K, Yu B, Chen S, et al. Heavy doping and band engineering by potassium to improve the thermoelectric figure of merit in p-type PbTe, PbSe, and PbTe 1- ySe y. J Am Chem Soc 2012;134:10031–8.

[15] Poudel B, Hao Q, Ma Y, Lan Y, Minnich A, Yu B, et al. High-thermoelectric performance of nanostructured bismuth antimony telluride bulk alloys. Science (80-) 2008;320:634–8.